Nanoscale properties of melting at the surface of semiconductors

Kerwyn Casey Huang,* Tairan Wang,[†] and John D. Joannopoulos

Center for Materials Science and Engineering, Massachusetts Institute of Technology, Cambridge, Massachusetts 02139, USA
(Received 18 July 2005; published 9 November 2005)

In this study, we use density-functional simulations to investigate how nanoscale surface coatings can alter the melting dynamics of semiconductor surfaces. We demonstrate that a single-monolayer coating of GaAs can dramatically reduce the diffusive motion of the surface atoms of a Ge(110) crystal and cause superheating of the bulk at temperatures well above the Ge melting point on the 10 ps time scale. In direct contrast, a single-monolayer coating of Ge will induce surface melting of a GaAs(110) structure 300 K below the GaAs melting point. We also identify a metallization of the band structure and bond alterations in the charge density near the melting transition. In addition, we suggest that the Ge monolayer causes the GaAs(110) surface to melt through transient penetration of the Ge atoms into the bulk, which locally initiates the collective diffusive motion of large groups of Ga and As atoms. These studies on the effect of coatings in semiconductors clearly point to the surface material as the dominant determinant of the melting characteristics of a hybrid structure. These simulations have important implications for high-temperature materials design while simultaneously probing the fundamental features of the melting transition.

I. INTRODUCTION

Despite our familiarity with the melting phase transition, a complete understanding of this complicated phenomenon has not yet been achieved.[1–6] Nevertheless, there are several unifying principles governing all melting behaviors. It has long been understood that melting is usually initiated by defects within the otherwise perfectly periodic crystal.[5] These defects can lie inside the bulk, such as point defects, line defects, and grain boundaries.[2,4,7,8] In addition, every experimental sample has inherent defects at the free surfaces,[6] where the crystal abruptly stops. The role of free surfaces in initiating melting has been studied both experimentally[9–11] and theoretically.[8,12,13]

Several sets of experiments have shown that the melting behavior of a substrate can be altered by thin (macroscopic) coatings of a different material. Daeges *et al.* have demonstrated that a Ag crystal coated with a ∼10–20 μm thick layer of Au can be superheated by 25 K for 1 min; by replacing the Ag-air interface with a Ag-Au interface, the core Ag material does not melt. Similar superheating behavior has also been observed in quartz (cristobalite) crystals surrounded by fused silica[9] and Ar bubbles in Al.[14] We note that in both cases, the dimensions of all components are macroscopic (at least tens of microns thick). Qualitatively, these experiments can be explained by the following argument: since the surface is known to play an important role in initiating melting, if the surface of a material with a lower melting point is coated with a material with a higher melting point, then the surface coating can maintain the core in a solid phase in some range of temperatures above the core melting point. At the molecular level, the coating will introduce a coherent interface that acts as a poor nucleation site for melting. However, to our knowledge, there has been no suggestion in the literature that superheating can be achieved with coating thicknesses below the micron scale. Morever, the choice of coating and substrate in the experiments discussed above is not arbitrary; it is only when the melting

point of the coating is higher than that of the substrate that a nucleation barrier to melting exists. The opposite construction, where the coating has a lower melting point than the substrate, has not been considered, either experimentally or theoretically.

To investigate the role played by the surface in the melting transition, we ask whether superheating and other dynamical phenomena are possible when the coating is only a *minimal* perturbation to the underlying surface.[13] Moreover, we investigate the possibility of the opposite phenomenon, in which such a minimal coating actually induces melting of the otherwise stable underlying surface. We will study the (110) surface of GaAs, which is the natural cleavage plane of GaAs, and the corresponding surface of Ge. Since the only significant difference between these semiconductors is their covalent or ionic bonding nature, a single monolayer of GaAs on Ge or vice versa can be considered a textbook example of how a coating could alter the melting behavior of a substrate. Given that the melting temperature of GaAs is higher than that of Ge by over 300 K, what might happen if Ge and GaAs coexist at a temperature in between their melting points? We approach this problem by examining the nanoscopic behavior of melting at the surface. In doing so, we intend to shed light on how one can control or alter the behavior of materials near the melting point, which could have implications for high-temperature materials applications.

The difference in melting points between Ge and GaAs is intriguing. Experimentally, Ge melts at $T_m(\text{Ge}) = 1211$ K, while GaAs remains solid until $T_m(\text{GaAs}) = 1540$ K.[15] Considering that Ga, Ge, and As are three consecutive elements in the Periodic Table, the ion masses are very similar, and in fact the average mass is nearly identical in Ge and GaAs. Furthermore, the two systems have almost identical lattice constant ($a = 1.07$ a.u.).[15] Thus, the largest difference between the two bulk materials is the bonding character. The tetrahedral bonds in Ge are fully covalent, while those in GaAs have some amount of ionic character.

Surprisingly, the formation enthalpy for Ge is 264 kJ/mol, more than 25% larger than that of GaAs at 210 kJ/mol. Thus, it takes less energy to "pull" a GaAs crystal apart than it takes to do the same to a Ge crystal. Yet, Ge melts at a temperature 300 K lower than what is necessary to melt GaAs. That is, there is less energetic cost to change Ge from solid to liquid than for GaAs, but more energetic cost to change Ge all the way to gas than GaAs.

On the (110) surface, another prominent difference between the two systems exists. The top-layer GaAs dimers buckle in such a way that the As atom moves away from the surface and its dangling bond is completely filled, while the Ga atom sinks into the surface with an empty dangling bond. The state of buckling in this case is determined by the bond energy difference between the dangling bonds of the surface Ga and As atoms. For the Ge surface, however, the two dangling bonds of the Ge dimer atoms are degenerate. Thus, the buckling involves a spontaneous symmetry breaking, and the energy difference of the resulting bonds is smaller than that of GaAs. Therefore, the Ge surface band gap is smaller and is easier to metallize, which we will suggest could be a prelude to melting.

In Sec. II, we describe the *ab initio* density-functional technique used to study the electronic structure of a surface at finite temperature. In Sec. III, we demonstrate that a coating of GaAs only a single monolayer in thickness can cause superheating in a Ge surface. We also explore how the band structure and charge density provides information about the timing and mechanisms of the melting transition.

In Sec. IV, we show that a single-monolayer coating of Ge can induce melting in a GaAs surface at a temperature well below the GaAs melting point. While coatings are generally considered to protect against melting by acting as barriers to defect nucleation, this study shows that surface coatings can actually initiate defect formation and ultimately lead to melting. In Sec. V, we use this Ge-coated GaAs system to suggest that melting is induced by surface atoms that have broken bonds with the rest of the surface layer penetrating into the bulk. Finally, in Sec. VI, we discuss potential sources of error and unanswered questions about melting at interfaces.

II. COMPUTATIONAL DETAILS

The simulations in this work utilize a molecular dynamics approach based on pseudopotential density-functional theory energy minimization. This approach is necessary to produce an accurate description of the motion of the Ga and As atoms. Furthermore, we reveal that the electronic structure information provides telltale signs that can help to identify the melting transition.

The time evolution of the system is determined according to the Born-Oppenheimer approximation,[16] separating the ion degrees of freedom from the electron degrees of freedom. During each time step, the ion locations are input into the electronic calculations, where density-functional theory (DFT) using the local density approximation[17] (LDA) is used to minimize the total electronic free energy and calculate the band structure. The forces on the ions are then calculated and the ions moved using classical molecular dynamics.

We update the positions of the ions using the Verlet algorithm,[18,19] which uses a standard discretization of Newton's equation,

$$m\frac{\partial^2 \mathbf{x}(t)}{\partial t^2} = \mathbf{F}(t) \Rightarrow \mathbf{x}_{i+1} = 2\mathbf{x}_i - \mathbf{x}_{i-1} + \frac{dt^2}{m}\mathbf{F}_i. \quad (1)$$

The temperature is maintained using an isokinetic molecular dynamics approach, in which the velocities are rescaled after each step to restore a fixed total kinetic energy. Our study follows the spirit of earlier work by Takeuchi *et al.*,[12] which used the same method to study the melting of the Ge(111) surface. The fact that we compare the relative differences in dynamics between two systems (with and without a coating) eliminates many of the errors due to supercell size, cutoff energy, time step, and ambiguities in the melting temperature, which can vary with system size and geometry.

Studies of melting using empirical potentials[20] can usually access a much longer time scale than corresponding quantum mechanical studies due to their lower computational requirements. For Si, there exist high quality three-body potentials such as those from Stillinger and Weber, which can reproduce a wide variety of physical properties, including melting dynamics.[21] However, for heteropolar materials such as GaAs, a high quality empirical potential which works well around the melting temperature has not yet been produced. As an added benefit to offset the increased computational costs of using DFT, the quantum mechanical treatment of the electrons allows us to analyze the electronic band structure and the charge density, in addition to ion trajectories. Previous work has shown that this additional information available from density-functional simulations can serve as a valuable tool for pinpointing the electronic transition from a solid to liquid phase.[12]

The computational supercells that we consider are composed of four free layers (18 atoms per layer) of either Ge or GaAs, capped by a frozen layer terminated with H atoms. The frozen layer is placed at $z=0$. To eliminate interactions between the top (surface) layer and the H layer in the cell above, the supercells are separated by $\sim$15 a.u. of vacuum.[12] In Sec. III, we compare the melting dynamics of the bare Ge(110) surface in Fig. 1(a) and the GaAs monolayer-coated surface [Ge(110)+GaAs] in Fig. 1(b). In Sec. IV, we compare the melting dynamics of the bare GaAs(110) surface in Fig. 1(c) and the Ge monolayer-coated surface [GaAs(110)+Ge] in Fig. 1(d).

The lattice constants a_x and a_y in the plane of the surface were chosen to be the same as the bulk values for the substrate. Before each simulation, the positions of the free atoms were relaxed. Simulations were performed using the freely available plane-wave density-functional code DFT++.[22] Unless otherwise noted, we have used the first 200 bands in the electronic iterations with a cutoff energy of 5 hartrees, and a time step of $dt=16$ fs for the ionic motion. Due to the large size of the supercell, it is only necessary to compute the density at the wave vector $k=\Gamma$. This has allowed us to study time scales of up to $\sim$12 ps, more than enough to compare melting behaviors in these surface structures. Indeed, Takeuchi *et al.*[12] have successfully studied surface melting very
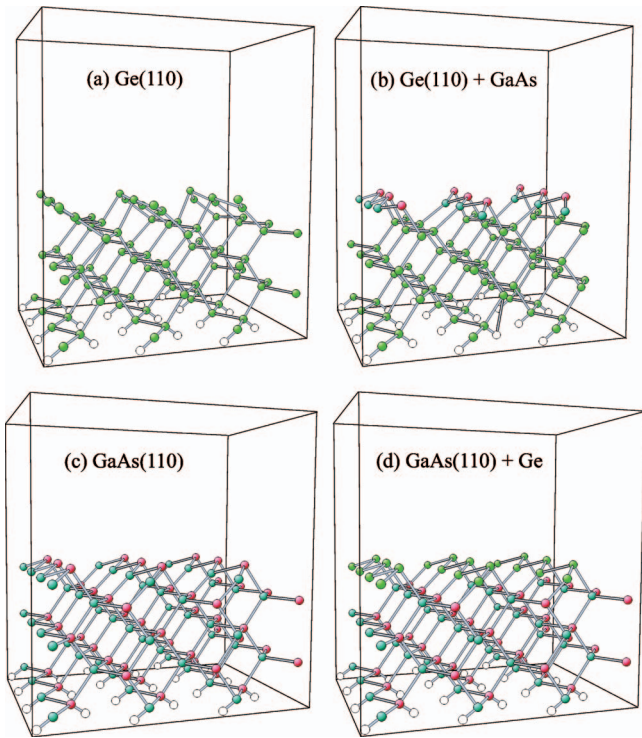
FIG. 1. (Color) Computational supercells: (a) the (110) surface of Ge [Ge(110)]; (b) the Ge(110) surface with a single-monolayer coating of GaAs [Ge(110)+GaAs]; (c) the (110) surface of GaAs [GaAs(110)]; and (d) the GaAs(110) surface with a single-monolayer coating of Ge [GaAs(110)+Ge]. Ge atoms are shown in green, Ga in blue, As in red, and H in white.

close to the melting point, where diffusive motion is far less pronounced (and thus harder to identify) than in our systems, using similar time scales and supercell sizes. Surface melting is the stage where the bulk material still exists in the solid

phase, while the surface of the material, due to its lower coordination, has already started the phase transition into liquid.

III. SUPERHEATING A GERMANIUM SURFACE

In this section, we compare the dynamics of a Ge surface to a similar structure where the top layer of Ge has been replaced by a GaAs monolayer. At temperatures between 1211 K and 1540 K, we expect that a bare Ge surface will go into a liquid phase rather quickly, while atoms on a GaAs surface should have very slight diffusion. Whereas the gold-on-silver experiments of Daeges *et al.* use coatings with ~60 000 layers,[11] we ask whether a *single-monolayer* coating can produce a significant change in the state of the surface and/or bulk. Similar to the gold-on-silver experiments, the GaAs-on-Ge arrangement could lead to a better resistance to melting in the Ge substrate by stabilizing the surface with the GaAs layer.

A. Ion trajectories

In Fig. 2, we plot the trajectories of the ions in each layer projected onto the (x,y) plane over a 10 ps period, starting with an equilibrium $T=0$ configuration. While there are still bond-breaking events in the GaAs monolayer and the two Ge layers below, it is clear that the motion of the Ge ions in the second, third, and fourth layers is dramatically slowed by the presence of the GaAs coating. Furthermore, the fourth layer appears to be more or less in the ideal crystal positions, as a solid. We will demonstrate that this is not an artifact caused by the frozen layer below.

A clear signal that distinguishes a melted liquid from an amorphous solid is the existence of normal diffusive motion, characterized by a linear increase in the mean-square displacement, $\langle \Delta R^2 \rangle$, as time progresses.[12] In the surface sys-
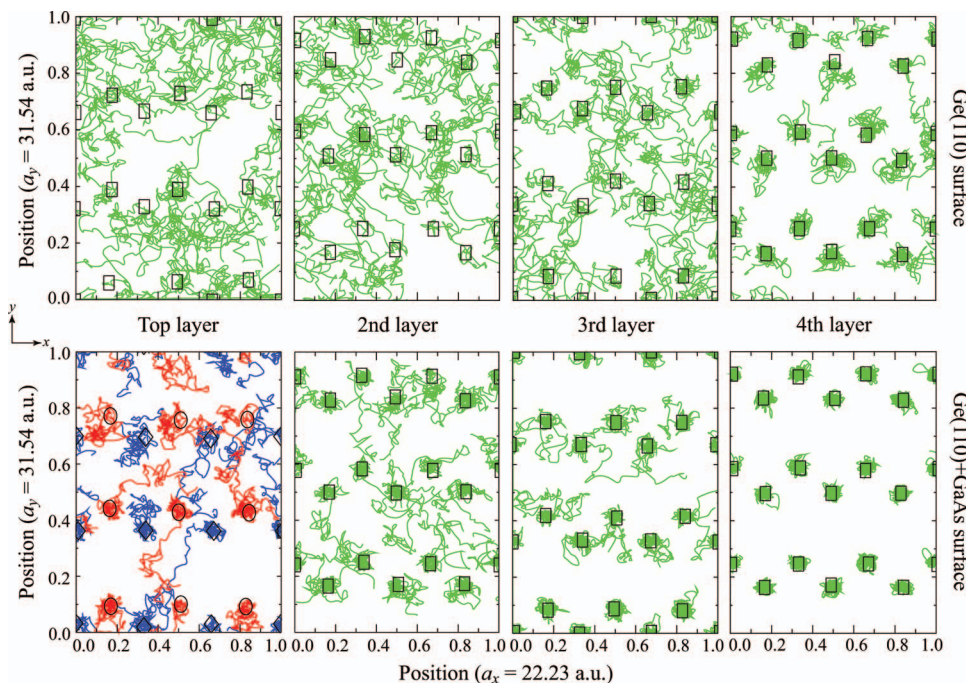

FIG. 2. (Color) Trajectories of the atoms on a Ge(110) surface at 1240 K for 10 ps, without (top) and with (bottom) a single-monolayer coating of GaAs, as they appear looking down the (110) direction. The ions are broken into groups based on their positions along the z axis (perpendicular to the surface) at $t=0$. Trajectories of Ga atoms are shown in blue, As in red, and Ge in green. The black diamonds (Ga), ovals (As), and rectangles (Ge) mark the initial positions of the atoms at $t=0$. Note the decrease in diffusive motion of the Ge atoms in the presence of a GaAs monolayer coating, especially in the fourth layer where melting is practically quenched.
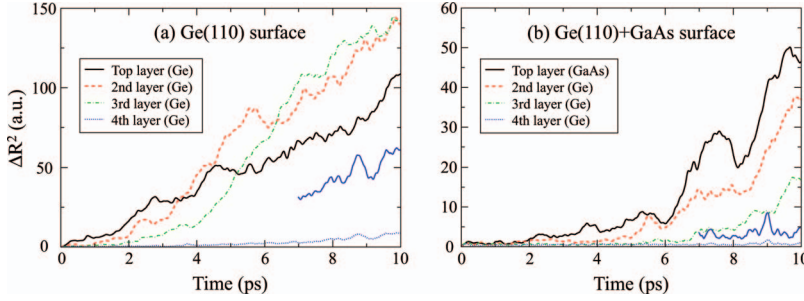
FIG. 3. (Color) Mean-square displacement $\langle \Delta R^2(t) \rangle$ averaged over the atoms within each of the top four layers of a Ge(110) surface at 1240 K (a) without and (b) with a monolayer coating of GaAs. The solid blue lines extending from $t = 7$ ps to $t = 10$ ps show $\langle \Delta R^2 \rangle$ for the fourth layer of atoms magnified by a factor of 5 to highlight the distinction between diffusive motion [linear $\langle \Delta R^2 \rangle$ in (a) and constant $\langle \Delta R^2 \rangle$ in (b)].

tems we have considered, the motion is primarily in planes normal to the surface, so we consider

$$\Delta R^2 = \Delta x^2 + \Delta y^2 \qquad (2)$$

and ignore the motion in the z direction for the purposes of calculating diffusion constants. In particular, we note that the GaAs coating and the underlying Ge layer do not form a mixture. In Figs. 3(a) and 3(b), we plot $\langle \Delta R^2 \rangle$ for the atoms in each layer of the bare and GaAs-coated Ge(110) surfaces, respectively. In agreement with Fig. 2, all four free layers of the Ge(110) surface appear liquid (linear $\langle \Delta R^2 \rangle$), indicating that 1240 K is above the melting point of our Ge(110) structure. In the GaAs-coated system, the GaAs monolayer and the first two underlying Ge layers have melted, but $\langle \Delta R^2 \rangle$ is roughly constant for the still solid fourth layer whose atoms are essentially vibrating about their initial positions. Thus, we conclude that we can achieve significant superheating in the fourth layer (and the remainder of the bulk) with a single-monolayer coating of GaAs. It is possible that with a larger supercell or longer time scales, the bulk would eventually melt as well. Regardless, this surface melting state is similar to the state observed on the Ge(111) surface by Takeuchi *et al.*[12] and represents a significant change from the rapid melting of the homogeneous Ge surface. We note that the gold-on-silver superheating results cannot be expected to extend to nanoscale coatings, since the ~ 10–20 μm coating of Au forms a mixture with the Ag subtrate with an extent roughly equal to the coating thickness.

The diffusion constant D_j for the atoms in a liquid layer j can be obtained from a fit to the equation

$$\langle \Delta R^2 \rangle_j(t) = 4D_j t, \qquad (3)$$

where $\langle \Delta R^2 \rangle_j$ indicates an average over ions. The factor of 4, rather than 6, in Eq. (3) is due to the fact that the diffusive motion is primarily two dimensional, as previously dis-

cussed. In Table I, we list the diffusion constants for each layer of the Ge(110) and Ge(110)+GaAs surfaces. At 1240 K, the diffusion constant of the Ge atoms in the second layer, D_2, is reduced by a factor of 2.4 by the GaAs coating, while D_3 is reduced by a factor of 4. In addition, we performed simulations of the two surfaces at 1270 K and 1540 K to test the effectiveness of the coating as a function of temperature. We observe similar significant reductions in the layer-by-layer diffusion constants in the presence of the GaAs coating at both temperatures, although the fourth layer begins moving diffusively by $T = 1270$ K.

At $T = 1240$ K, the contrast between the diffusive motion of the top three layers of the Ge(110)+GaAs surface and the nearly fixed positions of the atoms in the fourth layer prompts the question of whether this is an artifact due to the finite thickness of the slab and the fact that the bottom layer of Ge atoms is frozen in our simulation. To check if the atoms in the fourth layer are restricted in their motion because of their bonds with the fixed layer, we examine the total kinetic energies of each layer, converted to effective temperatures using the relation

$$KE_j = \sum_i \frac{1}{2} m_i v_{i,j}^2 = \frac{3}{2} k_B T_j, \qquad (4)$$

where $v_{i,j}$ is the velocity of atom i in layer j.

In Fig. 4, we observe that the effective temperatures T_j quickly reach equilibrium around the target of 1240 K. Thus, we conclude that although the fourth layer has far less mean-square deviation, these atoms have significant kinetic energy on par with the other layers. These atoms are moving vigorously despite the frozen layer below. Their motion is simply not diffusive like the layers above.

TABLE I. Diffusion constant averaged over the atoms in each layer, calculated from Eq. (3). Columns 2–5 correspond to the free layers of a Ge(110) surface, while columns 6–9 correspond to the free layers of a Ge(110)+GaAs surface. All quantities are given in units of 10^{-6} cm^2/s. There is no detectable diffusive motion in the fourth layer of the Ge(110)+GaAs surface at 1240 K, indicated in the table by the N/A symbol.

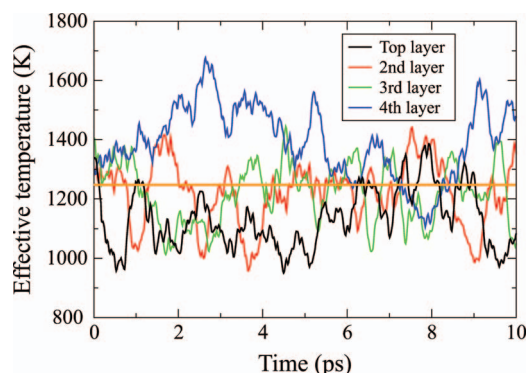| T (K)	Ge(110) surface				Ge(110)+GaAs surface			
	D_1^{Ge}	D_2^{Ge}	D_3^{Ge}	D_4^{Ge}	D_1^{GaAs}	D_2^{Ge}	D_3^{Ge}	D_4^{Ge}
1240	80	120	120	10	70	50	30	N/A
1270	90	80	120	10	130	80	40	2
1540	800	800	400	100	100	100	200	60

FIG. 4. (Color) The kinetic energy of the Ge(110)+GaAs surface at 1240 K (orange line), averaged over the atoms in each layer and converted to an effective temperature using Eq. (4).

B. Electronic signals of melting

While diffusion constants serve as a quantitative measure of the degree of melting, the time of phase transition is difficult to pinpoint in the ion trajectories. Previous attempts have been made to systematically identify the melting transition using electronic structure information. Phillpot *et al.* use the magnitude of the structure factor in each layer to identify the progression of melting from a defect in a crystalline system.[8] In addition, our *ab initio* density-functional calculations provide other information that can be used to pinpoint when melting occurs. Takeuchi *et al.* have also suggested that metallization of the band gap occurs when a crystal melts due to delocalization of the electrons as bonds are broken. In Fig. 5 we plot the band gap energy difference, $\Delta\omega$, between the highest conduction band and the lowest valence band at the Γ point for the Ge(110) and Ge(110) +GaAs surfaces. It is clear that the Ge(110) band gap disappears ($\Delta\omega[Ge] \lesssim 0.1 eV$) very quickly, indicating that the temperature is well above the melting point. In contrast, the band gap for the Ge(110)+GaAs surface slowly collapses over the first 6 ps. This collapse correlates with the reduction of diffusive motion of the Ge atoms in the two layers below
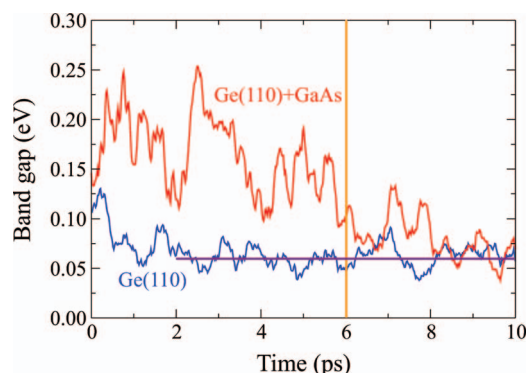

FIG. 5. (Color) The band gap energy in eV for the Ge(110) and Ge(110)+GaAs surfaces at 1240 K. Notice the collapse of the Ge(110)+GaAs band gap at $t \approx 6$ ps (orange line), signifying a change in character from semiconducting to metallic. The average Ge(110) band gap after $t=2$ ps, 0.06 eV, is marked by the horizontal, purple line.
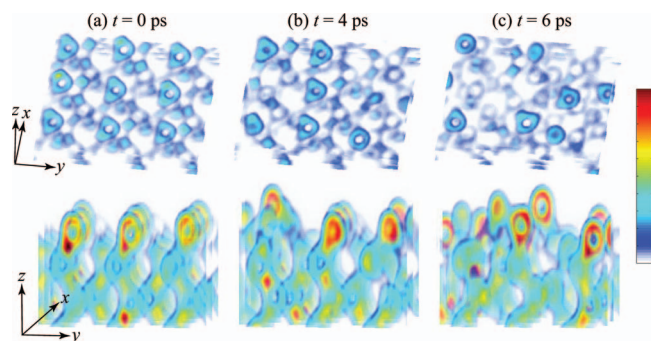

FIG. 6. (Color) Slices of the charge density of the Ge(110) +GaAs surface at (a) $t=0$ ps, (b) $t=4$ ps, and (c) $t=6$ ps. The top row of panels shows the view looking down the surface in the planes $z=1.8$, 5.1, 8.4, 11.6, 14.9 a.u. The bottom row of panels shows the side view looking down the x-axis in planes $x=0.5$, 4.2, 7.9, 11.6, 15.3, and 19 a.u. The planes are chosen by maximal average density. The color scheme is indicated on the right with maximum density in red and zero density in white.

the GaAs monolayer coating in Fig. 3. In addition, the diffusion constant of the top three layers in Fig. 3 appears to increase rapidly around $t=6$ ps. We note that the calculated band gap is smaller than expected due to use of the LDA and the existence of surface states.

To take a closer look at the electronic mechanism that initiates the collapse of the band gap, we study the charge distribution of the Ge(110)+GaAs system during the time period up to $t=6$ ps. Shown in Fig. 6 is the electron charge density in slices through planes of maximal average density perpendicular to the x and z axes before the run starts and after 4 and 6 ps. The time $t=4$ ps is chosen because this marks the approximate beginning of the linearity of $\langle\Delta R^2\rangle$ (see Fig. 3). There are few changes to the bottom free layer, so we focus on the top three layers. Comparing Figs. 6(a) and 6(b), many of the atoms in the first and second layers have reduced their coordination number from 3 and 4, respectively, to either 1 or 2. After 6 ps, close to the point of band gap collapse, many bonds are broken throughout the top three layers. In addition, the electrons are more spread out, which would explain the metallic behavior of the system.

Intuitively, we expect the level of superheating that can be achieved to decrease with increasing temperature, until eventually the GaAs coating ceases to provide sufficient resistance against the melting of the bulk. Where and how this transition occurs cannot be quantitatively addressed by our simulations due to the finite height of our supercell, but we have studied the Ge(110) and Ge(110)+GaAs surfaces at two other temperatures to get a rough idea of the deterioration of the coating performance. In Table I, we list the diffusion constants for each layer at $T=1240$, 1270, and 1540 K, the latter chosen since it is the experimental melting point of GaAs. There are several sources of error (see Sec. VI) that are increasingly important as T is increased. Nevertheless, our simulations show that when T reaches 1270 K, the third Ge layer beneath the GaAs coating begins to melt, and by the experimental melting temperature of GaAs at 1540 K, all Ge layers are thoroughly mixed in a liquid form. However, even
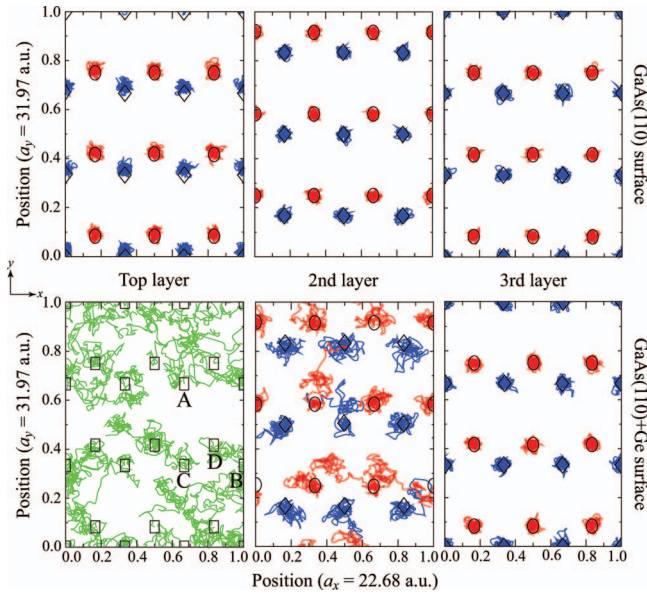
FIG. 7. (Color) Trajectories of the atoms in the top three layers of a GaAs(110) surface at 1240 K for 10 ps, without (top) and with (bottom) a single-monolayer coating of Ge, as they appear looking down the (110) direction. The color scheme is the same as in Fig. 2. Note how the Ge monolayer induces melting in the underlying layer of the GaAs crystal. The four atoms labeled A, B, C, and D are highlighted because they display significant motion in the z direction. The fourth layer of each system remains solid through $t = 10$ ps.

at 1540 K, all layers experience a noticeable reduction in diffusion constant compared to the bare Ge(110) surface. Ultimately, to study the superheating phenomenon at higher temperatures will require adding more free-moving layers to the bulk.

IV. INDUCED MELTING OF A GALLIUM ARSENIDE SURFACE

Given that the behavior of the Ge surface is so strongly regulated by the presence of a GaAs coating, we next ask what effect a single-monolayer coating of Ge will have on a GaAs surface. It is clear from Figs. 2 and 3 that a Ge surface will melt at 1240 K, but we expect that a GaAs surface would remain solid 300° below its melting point. Therefore, we entertain three possibilities for the behavior of a Ge-coated GaAs(110) surface: (i) the Ge coating will form a liquid monolayer on top of a solid GaAs bulk, (ii) the solid

TABLE II. Diffusion constant averaged over the atoms in each of the top two layers of the GaAs(110) and GaAs(110)+Ge surfaces, calculated from Eq. (3). All values are given in units of 10^{-6} cm^2/s. The third and fourth layers of the GaAs(110)+Ge surface and all layers of the GaAs(110) surface have a constant, rather than linear, $\langle \Delta R^2 \rangle$ vs t relationship (indicated in the table by the N/A symbol).

Layer	$D_{\mathrm{GaAs(110)}}$	$D_{\mathrm{GaAs(110)+Ge}}$
1 (GaAs/Ge)	N/A	40
2 (GaAs)	N/A	10

GaAs bulk will stabilize the Ge monolayer, or (iii) the Ge monolayer will become disordered and induce melting in the underlying GaAs surface.

In Fig. 7, we compare the trajectories of the ions in the top three layers of a bare GaAs(110) surface to the system where the top layer has been replaced by Ge atoms. We find that the ion dynamics is dominated by the character of the top layer, even more strongly than for the bare and GaAs-coated Ge(110) surfaces in Sec. III. As expected, the bare GaAs surface exhibits very little motion in any layer. This is in stark contrast to the coated GaAs(110)+Ge surface, where both the Ge atoms and the underlying layer of GaAs are highly diffusive. We have three reasons to believe that this induced melting phenomenon is not due to the formation of a mixture of Ge and GaAs with a lower melting point than pure GaAs. First, we have already observed that monolayer coatings do not form mixtures in the case of a GaAs monolayer on Ge(110). Second, the induced melting occurs at a temperature *far* below the GaAs melting temperature. Third, the fact that melting clearly propagates from the surface inwards, without significant exchange of atoms between the first and second layers, clearly indicates that this is a surface, rather than a mixture, effect. We will investigate this last piece of evidence in more detail in Sec. V.

As in Sec. III, we use the mean-square displacement, band structure, and charge density to study the details of the melting transition. In Fig. 8, we plot the average displacement of the atoms in the top four layers of each system. As expected, we find a constant $\langle \Delta R^2 \rangle$ for each layer of the bare GaAs(110) surface, signifying nondiffusive motion and a solid structure. However, $\langle \Delta R^2 \rangle$ increases linearly in time for the top two layers of the Ge-coated surface, with significant diffusion constants (see Table II). The third and fourth layers in each system remain solid up to $t = 10$ ps. This state of induced surface melting 300° below the melting point of GaAs is remarkable.
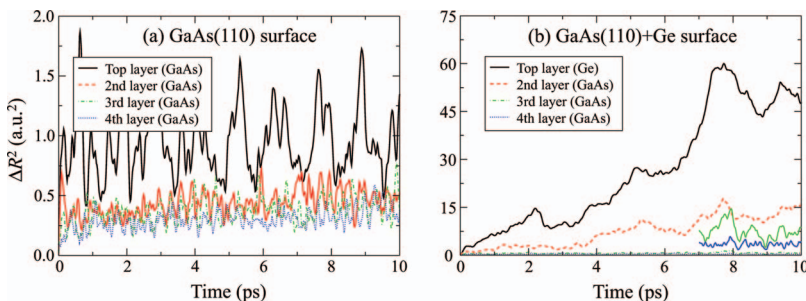

FIG. 8. (Color) Mean-square displacement $\langle \Delta R^2(t) \rangle$ averaged over the atoms within each of the top four layers of a GaAs(110) surface at 1240 K (a) without and (b) with a monolayer coating of Ge. Note the large difference in scales between (a) and (b). The solid blue and green lines in (b) extending from $t = 7$ ps to $t = 10$ ps show $\langle \Delta R^2 \rangle$ for the third and fourth layers of atoms, respectively, magnified by a factor of 10 to highlight the absence of diffusive motion.
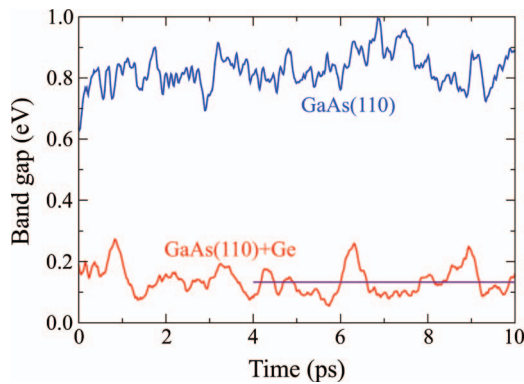
FIG. 9. (Color) The band gap energy in eV for the GaAs(110) and GaAs(110)+Ge surfaces at 1240 K. Note that neither band gap is completely collapsed on the 10 ps time scale. The horizontal, purple line indicates the average value of the GaAs(110)+Ge band gap from $t=4$ ps to $t=10$ ps (0.13 eV).

We plot the Γ-point band gap energy for the GaAs(110) and GaAs(110)+Ge surfaces in Fig. 9. The band gap is greatly reduced by the presence of a Ge-monolayer coating and shows signs of a slow collapse, although it does not consistently remain below 0.1 eV, as was found for the band gaps of the Ge(110) surfaces after 6 ps in Sec. III. This is probably a reflection of the stability of the third and fourth layers, although these layers may also melt at longer time scales.

In Fig. 10, the charge density through planes of maximal average density perpendicular to the z (top) and x (bottom) axes is shown at times $t=0$, 4, 8 ps. The top view shows the reduction in coordination number as bonds are broken and the electron density becomes more uniform. The side view indicates that the top two rows are becoming progressively disordered, while the third layer is relatively fixed in position with a higher degree of density localization. For the purposes of studying the melting process, the Ge monolayer and the first GaAs layer may be considered the only free-moving atoms of any significance. In this simplified system, only two atomic layers thick, we can isolate more easily the possible mechanisms of melting nucleation.
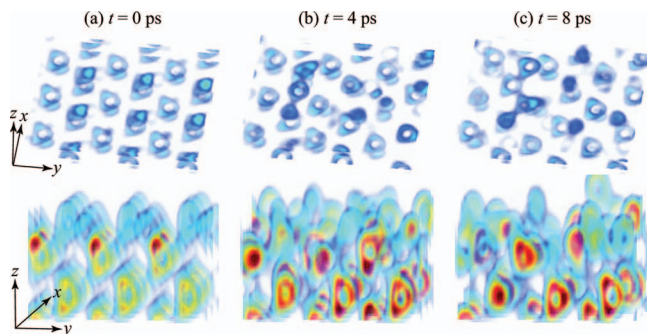

FIG. 10. (Color) Slices of the charge density of the GaAs(110)+Ge surface at (a) $t=0$ ps, (b) $t=4$ ps, and (c) $t=8$ ps. The top row of panels shows the view looking down the surface in the planes $z=1.5$, 4.4, 7.3, 10.2, and 13.1 a.u. The bottom row of panels shows the side view looking down the x axis in planes $x=0.5$, 4.3, 8.1, 11.8, 15.6, and 19.4 a.u. The planes are chosen by maximal average density.
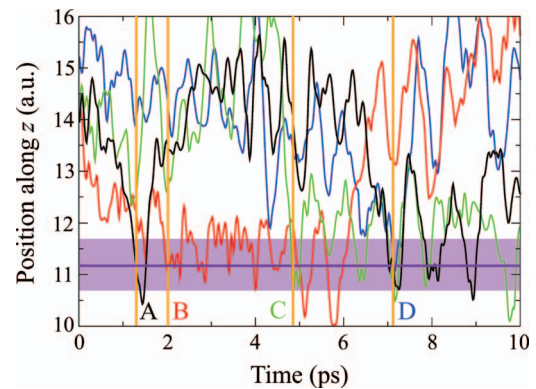

FIG. 11. (Color) The z component of the ionic coordinates of the four atoms in the surface monolayer coating of Ge on a GaAs(110) crystal that penetrate past the plane of the initial locations of the underlying layer of Ga and As atoms. The approximate extent of this layer of atoms is shown shaded in purple. The orange lines mark the times when atoms A, B, C, and D cross the plane $z=11.2$ a.u.

V. PENETRATION MECHANISM

Since the monolayer of Ge is clearly the direct cause of melting in Fig. 7, we investigate the role of bond breaking and penetration of surface atoms into the bulk in the propagation of the liquid-solid interface. The onset of diffusive motion of the Ga and As atoms in the underlying layer is precipitated by bond-breaking events in the Ge monolayer and the subsequent, transient penetration of several Ge atoms into the GaAs substrate.

In Fig. 11, we plot the z component of the ionic coordinates of the four Ge atoms, labeled A–D in Fig. 7, that penetrate past the initial position of the underlying plane of GaAs around $z=11.2$ a.u. during the 10 ps run. By $t=2$ ps, atoms A and B have broken away from the coating, and moved into the plane of the GaAs layer, shaded in purple in Fig. 11. Within 1 ps of entry, atom A quickly returns to the top Ge layer, while atom B remains until $t \sim 6$ ps. Atoms C and D remain a part of the surface layer until after $t=5$ ps. In Fig. 12, we plot the positions of these four atoms and the second-layer Ga and As atoms at $t=4$, 8 ps, represented as colored shapes as they appear looking up from inside the bulk, where larger shapes are atoms that are located farther into the bulk (decreasing z). The disorder in the GaAs layer is clearly nucleated locally around the penetration of atom B at $t=4$ ps, and the entire GaAs layer becomes more and more disordered as additional Ge atoms penetrate and interfere with the bonding structure. It appears that transient penetration of surface atoms, as opposed to permanent mixing with the underlying substrate, is enough to nucleate melting.

The motion of these four atoms perpendicular to the surface is clearly connected with the liquid dynamics of the second layer. It is easy to identify this penetration mechanism as the cause of melting in the coated GaAs structure due to the complete lack of melting in the bare GaAs structure, though this penetration mechanism is likely also the cause of melting in other structures. The increase in the magnitude of vibrations and subsequent melting from penetration
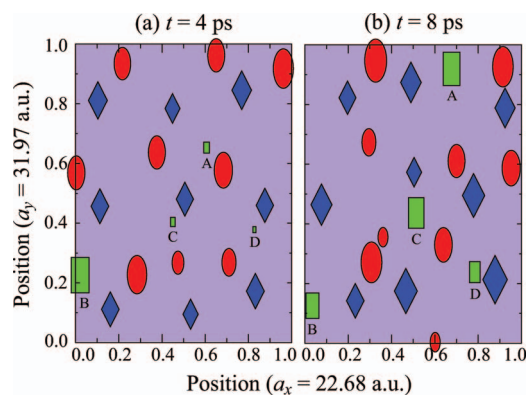
FIG. 12. (Color) The (x, y) positions of the Ga (diamonds) and As (ovals) atoms in the layer below the Ge coating of the GaAs(110)+Ge surface, as well as the Ge (rectangles) atoms A, B, C, and D marked in Figs. 7 and 11. The size of each atom is proportional to its penetration distance into the crystal. The largest object is at $z \approx 10$ a.u., the smallest is at $z \approx 16$ a.u. (a) At $t=4$ ps, atom A has transiently penetrated into the GaAs layer ($z \approx 11.2$ a.u.) and returned to the surface, while atom B remains in the second layer, disrupting the nearby Ga-As bonds in one row. (b) By $t=8$ ps, all four atoms have penetrated into the second layer and the distortion is widespread.

of surface atoms can also be understood within the context of the Lindemann criterion.[2] Furthermore, this mechanism also gives some indication of why the GaAs monolayer coating slows or stops the melting in the Ge layers of the Ge(110) +GaAs surface: none of the atoms in the upper three layers of this system penetrate within 2 a.u. of the initial plane of the fourth layer. Hence, this layer sees little intrusion from foreign atoms and consequently remains solid. It remains to be seen whether this system remains in a state of surface melting or increases in displacement of the ions in the second layer after $t=10$ ps result in subsequent melting of the third and fourth layers.

VI. DISCUSSION

Precise determinations of surface melting temperatures using DFT, such as those by Takeuchi *et al.*,[12] are highly dependent on the cutoff energy, supercell size, exchange-correlation functional, and choice of pseudopotentials. Considering all of these factors, an investigation of a single system's melting temperature is an involved affair, requiring careful studies at many temperatures for long time scales to ensure the stability of the solid below the theoretical determination of T_m. Although pseudopotential and finite-size errors cannot be ignored, the conclusions in this work are drawn from *comparisons* between similar structures that show how a monolayer coating can drastically alter the molecular dynamics of a surface. Because our simulations operate reasonably far away from T_m for any of the materials in the systems under comparison, many of the errors due to the factors mentioned above are likely to be systematic. Thus, the conclusions of superheating in Sec. III and induced melting in Sec. IV do not rely on a quantitative determination of the melting temperatures of the four structures in Fig. 1.

The results in this work are subject to several possible sources of error that are easily identified but inevitable due to limitations on computational resources. To test whether these sources of error have any qualitative effect on our results, we chose to examine the system with perhaps the most interesting dynamics, the Ge-monolayer coating on a GaAs surface, for any changes to our conclusion of induced surface melting.

An increase in the cutoff energy from 5 hartrees to 8 hartrees has little qualitative effect on the dynamics in Figs. 7 and 8. The diffusion constant of the second layer of atoms, D_2, remains equal to 10×10^{-6} cm^2/s. A reduction in the time step from 16 fs to 8 fs also had little effect on the surface melting ($D_2 \rightarrow 9 \times 10^{-6}$ cm^2/s). The effect of the finite size of each layer is likely to be most prominent along the direction with the most diffusion, the y axis (see Figs. 7 and 8). Doubling the lattice constant a_y from 32 to 64 a.u. also had no appreciable effect on the dynamics ($D_2 \rightarrow 8 \times 10^{-6}$ cm^2/s).

The setup of our structures also possesses an intrinsic source of error, namely the frozen layer with terminating H atoms at the bottom surface. When the Ge(110) surface melts, the propagation of the liquid-solid interface quickly hits this artificial, immobile bulk. Including additional layers (thereby increasing the supercell size in the z direction) and/or replacing the immobility of the frozen atoms with an average diffusivity or a continuum model will certainly have a quantitative effect on the diffusion constants in Tables I and II, and it may be possible to extend our results to more precise predictions about the electronic properties of the melting transition at temperatures very close to the melting point. However, the qualitative conclusions of superheating and induced melting from our simulations are readily apparent from the sharp changes in the dynamics of the four free layers caused by the application of a coating. In particular, it is clear from Fig. 3(a) that the frozen layer in the Ge(110) structure does not constrain or prevent melting in the atoms of the fourth layer directly above, whose diffusion constant is of the same magnitude as the top layer (see Table I), thus validating the appearance of superheating in the fourth layer of the Ge(110)+GaAs structure.

We have assumed vacuum conditions in the ~15 a.u. volume above the surface, since it is likely that foreign atoms and molecules such as H$_2$O will desorb at high temperatures. To verify this, we have performed simulations which predict the rapid desorption of H atoms from the GaAs(110)+Ge surface at 1240 K. Similar to Takeuchi *et al.*,[12] we have initiated each simulation run at the final temperature ($T =1240$ K, 1270 K, or 1540 K) to avoid the prohibitive computational costs in DFT of gradually increasing the temperature to mimic bulk heating. We again stress that because our main results involve comparisons of similar systems, any errors associated with this approach are likely to be systematic and therefore would not affect the occurrence of superheating or induced melting. (We note that different systems will have different time scales for thermalization and the onset of melting.) Thus, there is compelling evidence that a simple monolayer is sufficient to dramatically alter the melting behavior of a semiconductor surface. Similar studies with

other pairs of lattice-matched materials with a large difference in melting temperatures will help to validate our conclusions. The natural extension would be to heterostructures of InSb and Sn, whose lattice constants and average masses are equal but whose melting temperatures differ by almost $300°$ $[T_m(\text{InSb}=800 \text{ K}, T_m(\text{Sn})=504 \text{ K}].^{23}$ Fabrication of all of these systems is possible using molecular beam epitaxy.[24]

We have also implicated the penetration of isolated surface atoms in the initiation of layer-by-layer melting of the substrate. We hope to identify the precise dynamics which lead to the melting of individual layers through a series of simulations with a more accurate description of the electron density that also investigates the importance of stochasticity. In addition, further studies of larger supercells in a greater range of temperatures with longer time scales are required to discover how much superheating can be enhanced by increasing the coating thickness and its degradation at higher temperatures. We have focused on free surfaces, but larger supercells will also enable an analysis of the role of bulk defects in the melting process of GaAs heterostructures. Phillpot *et al.*[8] have investigated the nucleation of melting of Si at internal defects such as grain boundaries and dislocations. With further studies, we hope to answer whether the electronic structure of grain-boundary and dislocation-induced melting undergoes a similar transformation to the free surface.

In conclusion, we have provided evidence that the key feature that determines the melting behavior of a crystal is the composition of the surface. Using electronic-structure information and ion trajectories, we have described methods to identify the transition from a solid to a liquid state, and have suggested that the mechanism by which the melting occurs is dominated by transient penetration of surface atoms into the bulk, removing the nucleation barrier to melting. We have demonstrated that it may be possible to achieve superheating in a Ge crystal coated with a single monolayer of GaAs, a unique concept in semiconductors. In addition, we have shown that a single-monolayer coating of Ge can induce melting in an otherwise stable GaAs solid. It is tempting to consider that these phenomena can also be observed at other interfaces between materials with different melting points. The ability to ultimately control the melting point of semiconductors using nanoscale coatings promises to play an important role in the design of high temperature materials.

*Present address: Princeton University, Princeton, NJ 08540, USA. Electronic address: kchuang@princeton.edu

†Present address: Omniguide Communications, Inc., Cambridge, Massachusetts 02481, USA.

[1] A. R. Ubbelohde, *The Molten State of Matter: Melting and Crystal Structure* (Wiley, London, 1978).

[2] L. L. Boyer, Phase Transitions **5**, 1 (1985).

[3] R. M. J. Cotterill, E. J. Jensen, and W. D. Kristensen, Phys. Lett. **44**A, 127 (1973).

[4] R. M. J. Cotterill, J. Cryst. Growth **48**, 582 (1980).

[5] R. W. Cahn, Nature (London) **273**, 491 (1978).

[6] R. W. Cahn, Nature (London) **323**, 668 (1986).

[7] S. R. Phillpot, S. Yip, and D. Wolf, Comput. Phys. **3**, 20 (1989).

[8] S. R. Phillpot, J. F. Lutsko, D. Wolf, and S. Yip, Phys. Rev. B **40**, 2831 (1989).

[9] N. G. Ainslie, J. D. Mackenzie, and D. Turnbull, J. Phys. Chem. **65**, 1718 (1961).

[10] R. L. Cormia, J. D. Mackenzie, and D. Turnbull, J. Appl. Phys. **34**, 2239 (1963).

[11] J. Daeges, H. Gleiter, and J. H. Perepezko, Phys. Lett. A **119**, 79 (1986).

[12] N. Takeuchi, A. Selloni, and E. Tosatti, Phys. Rev. Lett. **72**, 2227 (1994).

[13] K. C. Huang, T. Wang, and J. D. Joannopoulos, Phys. Rev. Lett. **94**, 175702 (2005).

[14] C. J. Rossouw and S. E. Donnelly, Phys. Rev. Lett. **55**, 2960 (1985).

[15] C. Kittel, *Introduction to Solid State Physics*, 7th ed. (Wiley, New York, 1996).

[16] M. Born and J. R. Oppenheimer, Ann. Phys. **84**, 457 (1927).

[17] P. Hohenberg and W. Kohn, Phys. Rev. **136**, B864 (1964).

[18] L. Verlet, Phys. Rev. **159**, 98 (1967).

[19] L. Verlet, Phys. Rev. **165**, 201 (1967).

[20] S. R. Phillpot, S. Yip, and D. Wolf, Comput. Phys. **3**, 20 (1989).

[21] F. H. Stillinger and T. A. Weber, Phys. Rev. B **31**, 5262 (1985).

[22] S. Ismail-Beigi and T. A. Arias, Comput. Phys. Commun. **128**, 1 (2000).

[23] *Semiconductors: Group IV Elements and III-V Compounds*, edited by O. Madelung, Data in Science and Technology (Springer-Verlag, Berlin, 1991).

[24] A. Cho and J. Arthur, Physiol. Rev. **10**, 157 (1975).